HHS Public Access

Author manuscript

Biochemistry. Author manuscript; available in PMC 2019 December 26.

Published in final edited form as:

Biochemistry. 2018 December 26; 57(51): 6919–6922. doi:10.1021/acs.biochem.8b01046.

Mispacking of the Phe87 side chain reduces the kinetic stability of human transthyretin

Xun Sun, **Marcus Jaeger**, **Jeffery W. Kelly**, **H. Jane. Dyson**, and **Peter E. Wright***

Department of Integrative Structural and Computational Biology, Department of Chemistry, and Skaggs Institute of Chemical Biology, The Scripps Research Institute, 10550 North Torrey Pines Road, La Jolla, CA 92037, US.

Abstract

Aggregation of transthyretin (TTR) causes the TTR amyloidoses. The native TTR tetramer (a dimer of dimers) is stabilized by packing of phenylalanine 87 (F87) into a hydrophobic cavity of a neighboring protomer across the strong dimer-dimer interface. X-ray structures at acidic pH show that the side chain of F87 can be displaced from its binding pocket, but the resultant solution conformations remain unknown. Here we used ^{19}F-NMR and ^{19}F-labeled C10S-S85C TTR to characterize two local conformations of the loop containing F87. At neutral pH, F87 packs correctly into the inter-protomer cavity in the dominant conformational state (population 93%, T) whereas the remaining minor population is a mispacked tetramer (T*). The population of T* can be enhanced in heterotetramers by mixing C10S-S85C TTR with increasing molar ratios of A120L TTR, where a bulky leucine residue is introduced to disfavor the T state by steric hindrance.Exchange between the T and T* states in the presence of A120L is mediated by subunit exchange from the C10S-S85C tetramer. Compared to the TTR tetramer in which the dimers are correctly packed, mispacking of one or both dimer pairs leads to an increase of the urea-unfolding rate by 4-fold and at least 15-fold, respectively. Consistent acid-mediated tetramer dissociation was observed by ^{19}F-NMR aggregation assays. Our results highlight the important role of the inter-protomer F87 side chain packing in determining the kinetic stability of the TTR tetramer; mispacking of F87 in the T* state predisposes it for rapid dissociation and entry into the aggregation pathway.

Graphical Abstract

*Corresponding author: Peter E. Wright, wright@scripps.edu, Phone: 858 784 9721, Fax 858 784 9822.

ASSOCIATED CONTENT

Supporting Information. Methods and materials, supplementary tables showing the T* population and the three-state aggregation fits, and supplementary figures for ^{19}F-NMR spectra of F87A^{F}, different BTFA labeling sites, ^{19}F-NMR contour plots and peak areas, a cartoon illustrating the composition of the mixture, and turbidity assays. This supplementary material is available free of charge via the Internet at http://pubs.acs.org.

Notes

The authors declare no competing financial interest.

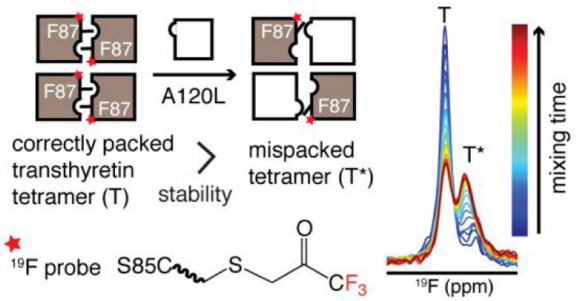

Human transthyretin (TTR, UniProtKB P02766), a homotetrameric protein found in plasma and cerebrospinal fluid, transports thyroxine and holo-retinol binding protein. The process of wild type (WT) TTR aggregation causes senile systemic amyloidosis, which affects ~25% of the population over age 80. The first step of TTR aggregation is dissociation of the TTR tetramer into a monomeric aggregation-prone intermediate,[1, 2] followed by an energetically favorable downhill self-assembly.[3] Accordingly, TTR amyloidogenicity is closely related to the thermodynamic and kinetic stabilities of the TTR tetramer.[4, 5] Amino acid point mutations that weaken the native TTR tetramer result in familial TTR amyloidosis due to mutant TTR aggregation with an earlier age of onset.[6, 7]

The native TTR tetramer is a dimer of dimers. Each monomer consists of a β-sandwich of two four-stranded β-sheets comprising the DAGH and CBEF strands. The antiparallel arrangement of the H-H' strands (residue 115–123) extends the DAGH sheet across neighboring subunits and forms the primary basis of the strong dimer interface whereas the AB and GH loops (residue 18–27 and 112–115) from two protomers pack against each other in the weak dimer interface. Among the molecular interactions that stabilize the TTR tetramer at the strong dimer interface, the side chain of F87 packs into a hydrophobic pocket in the neighboring protomer (red spheres in Figure 1A, B), formed by the side chains of several residues including A120 (orange spheres in Figure 1B). Interestingly, an alternative local conformation of the EF loop (residue 81–91) has been reported based on an X-ray structure at pH 4.0, where F87 is dislodged from the cavity (magenta spheres in Figure 1A, B).[8] However, how the side chain packing of F87 affects the conformational stability of the TTR tetramer in solution is unknown.

Previously we reported that quantitative labeling of TTR with 3-bromo-1,1,1-trifluoroacetone (BTFA) at a site adjacent to the strong dimer interface (S85C) provides a sensitive probe to report on the populations of tetramer and monomer during aggregation.[10] BTFA labeling does not perturb the TTR structure nor its aggregation kinetics. Based on the proximity of the BTFA probe to F87, we reasoned that the same probe could report on local conformational changes in the EF loop. In the present study, we employ ^{19}F-NMR to directly visualize two solution conformations associated with differences in F87 side chain packing. To modulate their relative populations, we introduced steric hindrance for the F87 sidechain by mutation of A120 inside the inter-protomer cavity. Our results indicate that mispacking of the F87 side chain leads to reduced kinetic stability, as ascertained by urea unfolding and acid-mediated tetramer dissociation.

Figure 1C shows a ^{19}F-spectrum of C10S-S85C-BTFA (TTR^F) at pH 7.0 and 298 K. A minor shoulder resonance (T*) is observed, with a population of 7 ± 1 % (estimated from the fitted Lorentzian peak areas and averaged from four independently expressed batches of TTR). This peak is upfield-shifted by 0.08 ppm from the major tetramer peak (T) at −84.18 ppm. The stoichiometric labeling by BTFA excludes the possibility of multiple labels on one TTR protomer and is specific to S85C as a cysteine-free C10S construct is not labeled by BTFA under the same conditions.[10] The population and the ^{19}F chemical shift of T* remain unchanged in C10A-S85C-BTFA, which suggests that the mutation of C10 does not affect the relative population of T* and T. ^{19}F longitudinal diffusion-ordered NMR spectroscopy (DOSY)[11] confirmed that T* is a tetramer (Figure 1D), whose relative population is invariant over a TTR concentration range of 10 to 360 μM (monomer concentration; Table S1). The ^{19}F-NMR spectrum of the C10S-S85C-F87A-BTFA ($F87A^F$) mutant exhibits only one tetramer resonance at −84.17 ppm and no signal corresponding to the T* state (Figure 1C), suggesting that the minor (T*) tetramer conformation in TTR^F is likely linked to F87. Due to the destabilization caused by F87A, a new peak appears at −84.48 ppm that is assigned to the $F87A^F$ monomer. The relative intensity of the monomer peak (M) is enhanced at the cost of the downfield tetramer resonance (T) by dilution (Figure S1A) and by decreasing the temperature to weaken the hydrophobic interaction that stabilizes the TTR tetramer more than the monomer (Figure S1B). The assignment of the $F87A^F$ monomer resonance was further substantiated by the similar ^{19}F chemical shift of the monomeric TTR^F aggregation intermediate at −84.47 ppm.[10] Proximity of the BTFA reporter to F87 is necessary to distinguish T and T*; only one symmetric ^{19}F resonance was observed for C10S-S46C-BTFA and C10S-E63C-BTFA, where the probes were placed far away from F87 (Figure S2). Further, the absence of the T* peak from these spectra rules out the possibility that the minor species observed for TTR^F might arise from coupling of BTFA at a secondary site.

The upfield ^{19}F chemical shift of T* in the spectrum of TTR^F and the absence of the T* resonance from the spectrum of $F87A^F$ support the notion that the local environment of the EF loop is more solvent-exposed in T*[12] and that F87 is involved in this conformational change. We hypothesized that the major conformation T corresponds to a correctly packed tetramer, with the F87 side chain inserted into its docking site on the neighboring protomer, and that T* arises from a mispacked subunit interface. To test this hypothesis, we introduced a conformational bias to favor the energetically unfavorable T* state at the cost of T. Since the side chains of A120 and F87 are tightly packed (Figure 1B), we created an A120L mutant where a bulky leucine was introduced to displace the F87 side chain from its correct docking site by steric hindrance. Indeed, mixing 10 μM TTR^F and 80 μM A120L over 66 h at pH 7.0 and 298 K enhances T* and reduces T simultaneously (Figure 2A, S3A). The total peak areas of T and T* are conserved (Figure S4A) showing that T and T* inter-convert in the presence of A120L. The relative population of T* is positively correlated with the molar ratio of A120L:TTR^F (Figure 2B). The T–T* exchange rate was measured as 0.038 ± 0.003 h^{-1} (Figure 2C); this rate is largely determined by subunit exchange from TTR^F. At the mixing concentration (80 μM), A120L is a mixture of monomer and tetramer (SI text). Upon (slow) dissociation of a subunit from the TTR^F tetramer, the excess A120L monomer is rapidly incorporated to form a heterotetramer. The presence of A120L is necessary to drive

the population shift as no changes in the population of T* occur in the absence of A120L (Figure 2D, S3B, S4B).

Having confirmed the mispacking of F87 in T*, we next characterized its kinetic stability using urea unfolding. The unfolding rate for the T resonance of TTR^F at pH 7.0, 298 K in 6 M urea (Figure S3C, S4C) is 0.066 ± 0.001 h^{-1}, which closely matches the rate predicted (0.067 h^{-1}, see SI text) from the subunit exchange rate for TTR^F alone (0.038 h^{-1}, Figure 2C) and the reported urea-dependence of the tetramer dissociation rate for WT TTR.[4] This comparison, and the fact that TTR^F and WT TTR have the same subunit exchange rates (~0.038 h^{-1} at pH 7.6 and 298 K)[13], establishes that TTR^F and WT TTR have similar kinetic stabilities at neutral pH. The small population of T* in TTR^F, however, renders kinetic quantification challenging as it disappears into the noise within 1 h in 6 M urea (Figure S3C). To measure the unfolding kinetics of T*, we therefore increased its population by incubating A120L and TTR^F (8:1 mole ratio) to form mixed heterotetramers prior to urea unfolding (Figure S3D). The expected composition of the heterotetramers is illustrated in Figure S5. Remarkably, the majority of the T* state, which arises from heterotetramers without any correctly packed dimers, is unfolded within 1 h (k_{obs} > 1 h^{-1}), leading to an amplitude burst in the unfolded resonance (U) that is upfield shifted by 0.09 ppm from T* (Figure 3A). The decay rate of the T resonance, which is associated with a heterotetramer with only one pair of correctly packed dimers (Figure S5), is 0.26 h^{-1}, 4 times faster than that of the T state of the TTR^F tetramer with two correctly packed dimer pairs (Figure 3B).

Consistent with the rapid unfolding of T* in the hybrid tetramer, the T* resonance nearly completely disappears within 1 h after the pH is lowered from 7.0 to 4.4 at 298 K (Figure 3C, S3E). Moreover, the T state of the heterotetramer dissociates into a monomeric, aggregation-prone intermediate (I) more quickly than T in TTR^F alone (Figure 3D). Unlike the constant ^{19}F NMR signal amplitude in urea unfolding (Figure S4C, S4D), the overall signal amplitudes of T and I decay over time (Figure S4E), showing the formation of NMR-invisible aggregates (A). Fitting the aggregation data using a three-state model $(T \underset{k_{-1}}{\overset{k_1}{\rightleftharpoons}} I \underset{k_{-2}}{\overset{k_2}{\rightleftharpoons}} A)$ [10] shows that both the tetramer dissociation rate (k_1) and monomer tetramerization rate (k_{-1}) increase by 12-fold for the heterotetramer, compared to TTR^F alone (Table S2).

The kinetic trace of the I species of TTR^F with premixed A120L reaches a maximum at 0.4 h, sooner than TTR^F alone (~6 h, Figure 3D). Moreover, the decay of the I resonance is much faster with premixed A120L, and its steady state level (3%) is lower than that for TTR^F alone (8%). These changes are reflected in a 16-fold increase in the oligomerization rate (k_2) that consumes the I species. For comparison, the increase in the reverse oligomerization rate k_{-2} is only about 3-fold (Table S2). The greater increase of the oligomerization rate is likely due to the presence of excess A120L, which could co-aggregate with the TTR^F I species. Consistent with this idea, the $t_{1/2}$ in turbidity assays decreases from ~49 h for TTR^F alone (10 μM) to ~15 min for the A120L:TTR^F (80:10 μM) mixture (Figure S6).

Conformational changes around the EF loop have been associated with TTR aggregation at mildly acidic pH.[8, 14] Not only is the EF loop adjacent to the strong dimer interface, it also packs against the AB and GH loops in the weak dimer interface. One pathogenic mutation in this region, I84S, is highly aggregation-prone[15] and the X-ray structure shows local unfolding of the EF helix as well as an altered conformation of the EF loop.[16] In addition, the backbone amides in the EF loop are severely broadened by exchange in a monomeric TTR at low pH.[14] In the same vein, the ^{19}F transverse relaxation rate constant (R_2) is larger for T* (42 s^{-1}, see SI text) than for T (28 s^{-1}), indicating that T* is more conformationally dynamic than T. Collectively, these results suggest that the local conformational dynamics of the residues in the EF loop could drive the amyloidogenic misassembly of the monomeric aggregation intermediate.

In conclusion, by combining ^{19}F-NMR analysis with a mutation (A120L) designed to introduce steric hindrance into the strong dimer interface, we show that the two solution conformations of the TTR tetramer, T and T*, are associated with differences in side chain packing of F87 and that their relative populations can be modulated by mixing with A120L protomers. The kinetic stability of the heterotetramers with mispacked dimers is reduced as compared to the tetramer with both dimers correctly packed. Our results show the important role of F87 side chain packing on stabilizing the TTR tetramer against local conformational fluctuations and self-aggregation. Exploring alternative molecular markers to monitor conformational changes in this key region of TTR is currently underway.

Supplementary Material

Refer to Web version on PubMed Central for supplementary material.

ACKNOWLEDGMENT

We thank Gerard Kroon for assistance with NMR experiments and Euvel Manlapaz for technical support.

Funding

This work was supported by National Institutes of Health Grant DK34909 (to P.E.W.), the Skaggs Institute for Chemical Biology, and American Heart Association Grant #17POST32810003 (to X.S.).

REFERENCES

1. Quintas A, Saraiva MJ, and Brito RM (1999) The tetrameric protein transthyretin dissociates to a non-native monomer in solution. A novel model for amyloidogenesis, J. Biol. Chem 274, 32943–32949. [PubMed: 10551861]
2. Lai Z, Colon W, and Kelly JW (1996) The acid-mediated denaturation pathway of transthyretin yields a conformational intermediate that can self-assemble into amyloid, Biochemistry 35, 6470–6482. [PubMed: 8639594]
3. Hurshman AR, White JT, Powers ET, and Kelly JW (2004) Transthyretin aggregation under partially denaturing conditions is a downhill polymerization, Biochemistry 43, 7365–7381. [PubMed: 15182180]
4. Hammarstrom P, Jiang X, Hurshman AR, Powers ET, and Kelly JW (2002) Sequence-dependent denaturation energetics: A major determinant in amyloid disease diversity, Proc. Natl. Acad. Sci. U.S.A 99 Suppl 4, 16427–16432. [PubMed: 12351683]

5. Sekijima Y, Wiseman RL, Matteson J, Hammarstrom P, Miller SR, Sawkar AR, Balch WE, and Kelly JW (2005) The biological and chemical basis for tissue-selective amyloid disease, Cell 121, 73–85. [PubMed: 15820680]

6. Connors LH, Lim A, Prokaeva T, Roskens VA, and Costello CE (2003) Tabulation of human transthyretin (TTR) variants, 2003, Amyloid 10, 160–184. [PubMed: 14640030]

7. Johnson SM, Connelly S, Fearns C, Powers ET, and Kelly JW (2012) The transthyretin amyloidoses: From delineating the molecular mechanism of aggregation linked to pathology to a regulatory-agency-approved drug, J. Mol. Biol 421, 185–203. [PubMed: 22244854]

8. Palaninathan SK, Mohamedmohaideen NN, Snee WC, Kelly JW, and Sacchettini JC (2008) Structural insight into pH-induced conformational changes within the native human transthyretin tetramer, J. Mol. Biol 382, 1157–1167. [PubMed: 18662699]

9. Peterson SA, Klabunde T, Lashuel HA, Purkey H, Sacchettini JC, and Kelly JW (1998) Inhibiting transthyretin conformational changes that lead to amyloid fibril formation, Proc. Natl. Acad. Sci. U.S.A 95, 12956–12960. [PubMed: 9789022]

10. Sun X, Dyson HJ, and Wright PE (2018) Kinetic analysis of the multi-step aggregation pathway of human transthyretin, Proc. Natl. Acad. Sci. U.S.A 115, E6201–E6208. [PubMed: 29915031]

11. Altieri AS, Hinton DP, and Byrd RA (1995) Association of biomolecular systems via pulsed field gradient NMR self-diffusion measurements, J. Am. Chem. Soc 117, 7566–7567.

12. Sun X, Dyson HJ, and Wright PE (2017) Fluorotryptophan incorporation modulates the structure and stability of transthyretin in a site-specific manner, Biochemistry 56, 5570–5581. [PubMed: 28920433]

13. Rappley I, Monteiro C, Novais M, Baranczak A, Solis G, Wiseman RL, Helmke S, Maurer MS, Coelho T, Powers ET, and Kelly JW (2014) Quantification of transthyretin kinetic stability in human plasma using subunit exchange, Biochemistry 53, 1993–2006. [PubMed: 24661308]

14. Lim KH, Dyson HJ, Kelly JW, and Wright PE (2013) Localized structural fluctuations promote amyloidogenic conformations in transthyretin, J. Mol. Biol 425, 977–988. [PubMed: 23318953]

15. Miller SR, Sekijima Y, and Kelly JW (2004) Native state stabilization by NSAIDs inhibits transthyretin amyloidogenesis from the most common familial disease variants, Lab. Invest 84, 545–552. [PubMed: 14968122]

16. Pasquato N, Berni R, Folli C, Alfieri B, Cendron L, and Zanotti G (2007) Acidic pH-induced conformational changes in amyloidogenic mutant transthyretin, J. Mol. Biol 366, 711–719. [PubMed: 17196219]

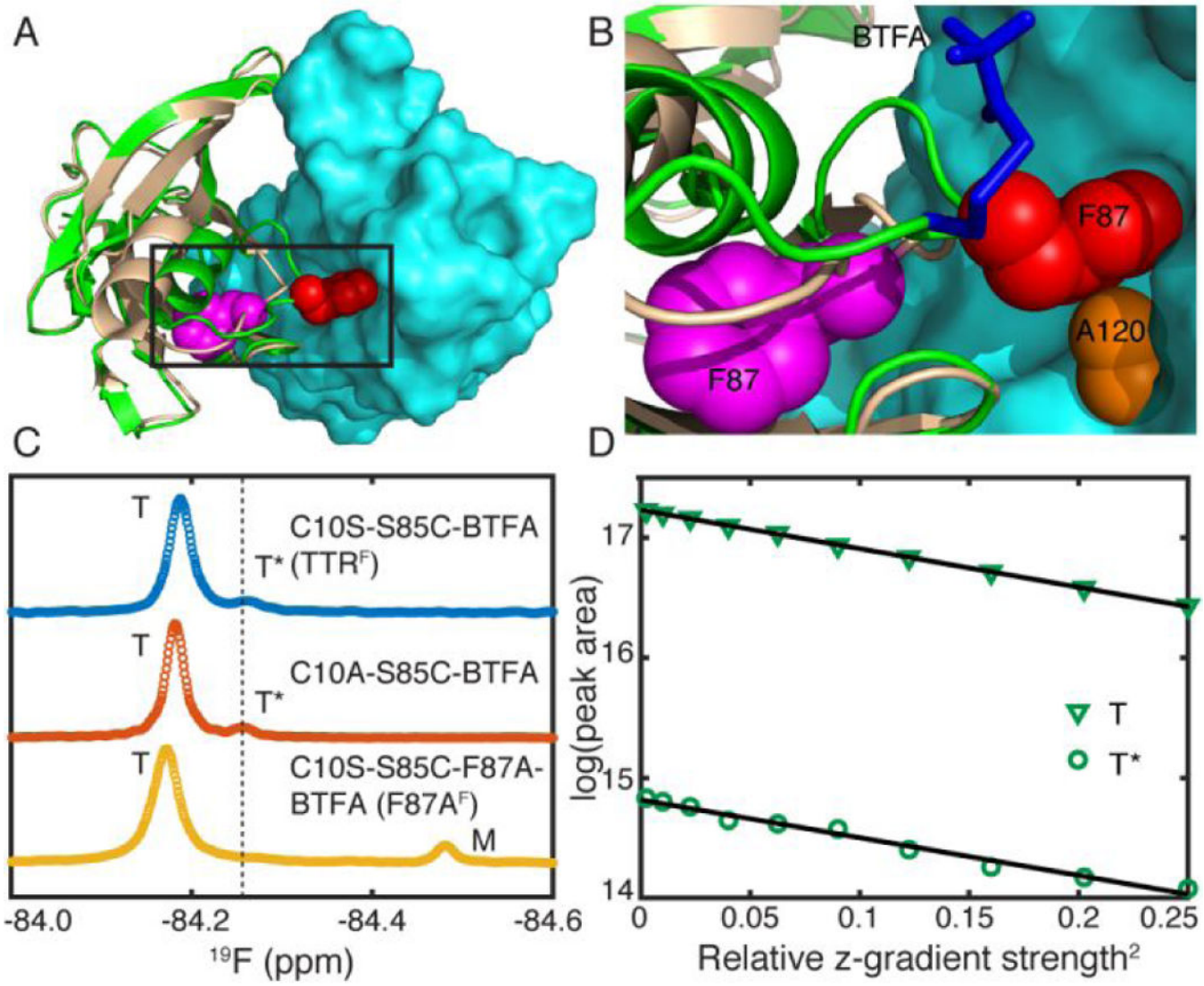

Figure 1.

(A) Two TTR X-ray structures (green/cyan: 1BMZ[9] and tan/cyan: 3D7P[8]), aligned using the cyan protomer, showing the distinct local conformations around F87. The heavy atoms of F87 side chains are shown in red and magenta spheres for the green and tan TTR, respectively. (B) Close-up showing packing of the red F87 side chain into a hydrophobic cavity in the adjacent (cyan) protomer; A120 in the cyan protomer is colored orange. The ^{19}F-BTFA probe at S85C was modeled according to Ref[10] and is shown as blue sticks. (C) ^{19}F-NMR spectra of C10S-S85C-BTFA (TTR^{F}), C10A-S85C-BTFA and C10S-S85C-F87A-BTFA (F87A^{F}). The major tetramer, minor tetramer and monomer species are labeled as T, T* and M. (D) ^{19}F-DOSY data for C10A-S85C-BTFA has the same slope for T and T* (slope ratio 1.02 ± 0.05) showing that the translational diffusion coefficients are the same and hence that both species are tetrameric. Black lines denote linear fits.

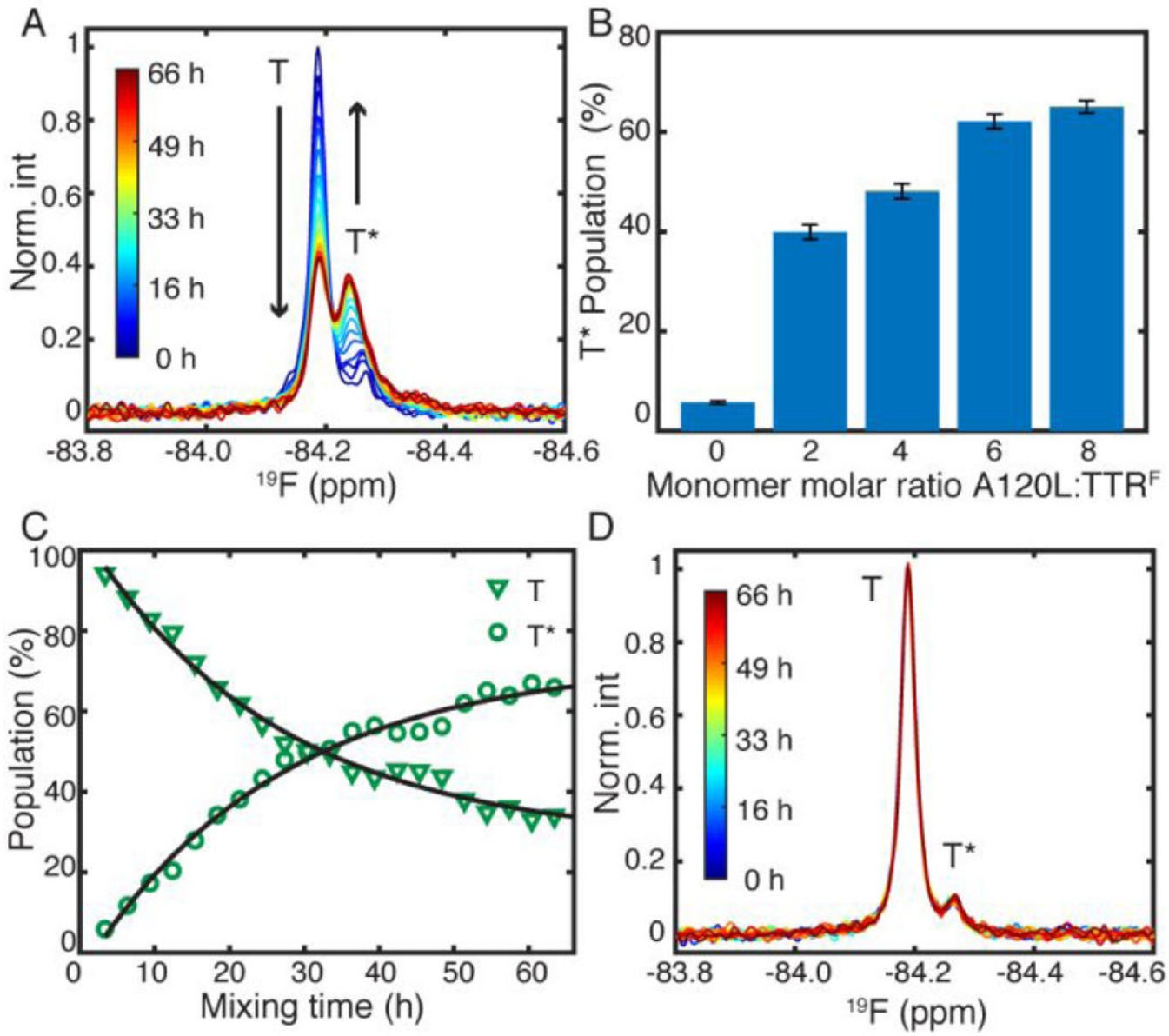

Figure 2.

(A) Changes in peak intensity with time following mixing of A120L and TTR^{F} at pH 7.0, 298 K. in an 8:1 monomer ratio. (B) The post-mixing population of T* as a function of the A120L:TTR^{F} molar ratio. The uncertainty was calculated as one standard deviation from 50 bootstrapped datasets. (C) Exchange kinetics determined from single exponential fits of the intensity changes in (A). (D) The relative populations of T* and T in TTR^{F} remain constant in the absence of A120L.

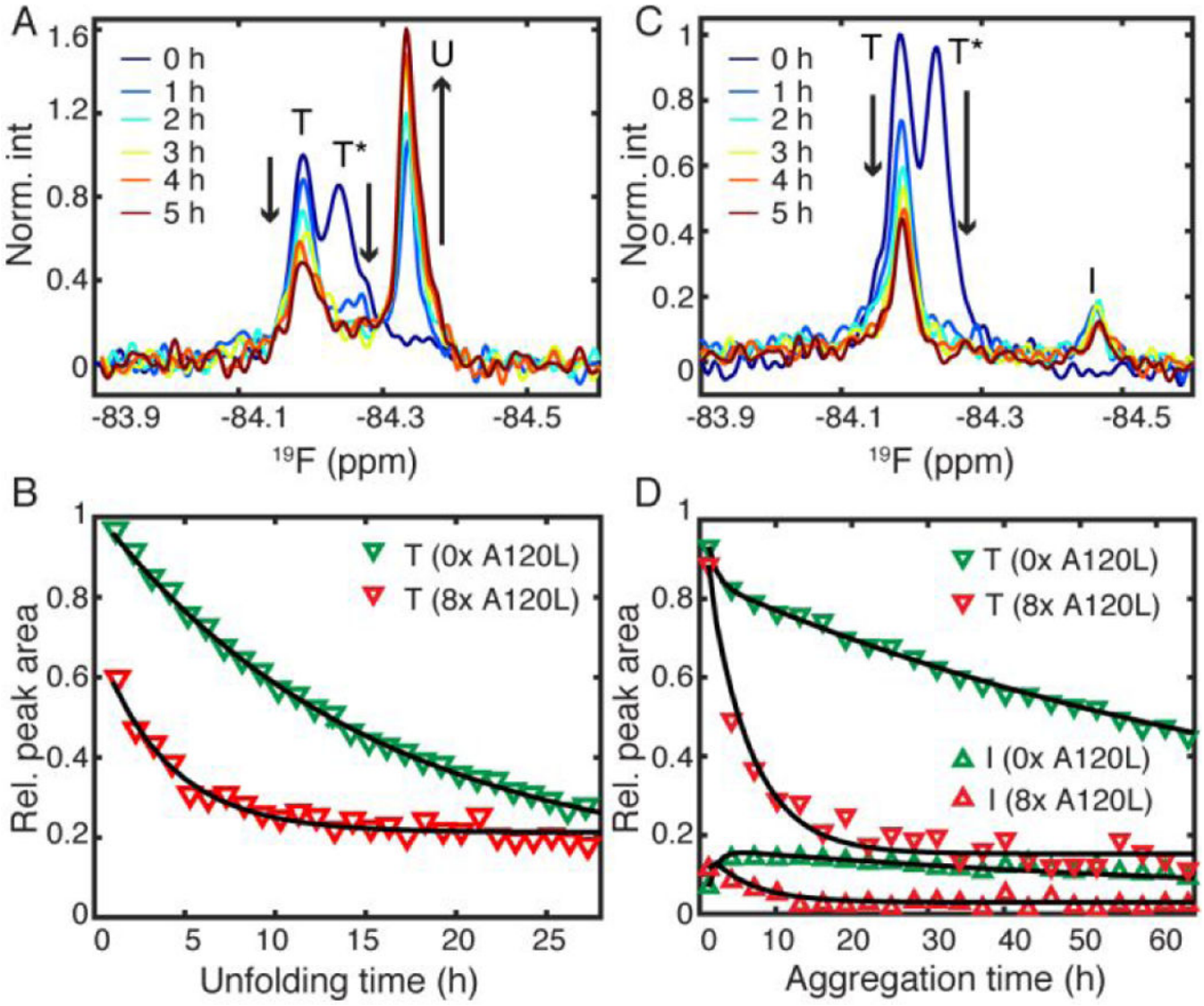

Figure 3.

(A) ^{19}F-NMR spectra before and after unfolding by 6 M urea. (B) Unfolding kinetics of T with 8-fold A120L (A) in red and without premixed A120L (green). Black lines are single exponential fits. (C) Acid-mediated aggregation of TTR^F premixed with 8-fold A120L. (D) The aggregation kinetics of T and I in (C) are shown in red. For comparison, the aggregation data of TTR^F alone are plotted in green.[10] Black lines are fits from a three-state kinetic model (see main text).